NATIONAL ADVISORY COMMITTEE FOR AERONAUTICS

TECHNICAL NOTE 2786

EQUIVALENT PLATE THEORY FOR A STRAIGHT MULTICELL WING

By Stanley U. Benscoter and Richard H. MacNeal

California Institute of Technology

Washington
September 1952

1K

NATIONAL ADVISORY COMMITTEE FOR AERONAUTICS

TECHNICAL NOTE 2786

EQUIVALENT PLATE THEORY FOR A STRAIGHT MULTICELL WING

By Stanley U. Benscoter and Richard H. MacNeal

SUMMARY

A structural theory is developed for the analysis of thin multicell wings with straight spars and perpendicular ribs. The analysis is intended to be suitable for supersonic wings of low aspect ratio. Deflections due to shearing strains are taken into account. The theory is expressed entirely in terms of first-order difference equations in order that analogous electrical circuits can be readily designed and solutions obtained on the Cal-Tech analog computer.

INTRODUCTION

In the process of designing thin supersonic wings for minimum weight it is found that a convenient construction with aluminum alloy consists of a rather thick skin with closely spaced spars and no stringers. Such a wing deflects in the manner of a plate rather than as a beam. Internal stress distributions may be considerably different from those given by beam theory, particularly for torsional or eccentric loading.

A thin-walled multicell wing may be regarded as an elastic shell in which the webs, or wall segments, act as membranes. By introducing appropriate simplifying assumptions it is possible to reduce the equations for such a shell to the form of plate equations provided that one simple criterion is satisfied. The chordwise cross sections must have a horizontal axis of symmetry. This condition is usually satisfied in supersonic wings which do not contain stringers.

The theory which has been developed is of the simplest form that could be reasonably expected to give results of an accuracy that would be satisfactory for engineering purposes. The loading is assumed to consist of a set of vertical concentrated forces acting at the intersections of the ribs and spars. The distributed load on the wing must be replaced, in some rational manner, by an equivalent set of concentrated loads.

In order that a solution may be obtained on an analog computer, the structural theory is expressed entirely in terms of first-order

difference equations. The design of the analogous electrical circuit is explained and illustrated.

This paper was prepared at the California Institute of Technology under the sponsorship and with the financial assistance of the National Advisory Committee for Aeronautics.

SYMBOLS

A_r	area of rib (shear web only)
A_s	area of spar (shear web only)
a,b,c,d	components of displacement which midpoints of a panel take when panel is put in shear
C	shearing stiffness of a spar or rib
D	bending or twisting stiffness of an element
$D_{ij}' = \lambda_i \mu EI/(1 - \mu^2)$	
$D_{ji}' = \lambda_j \mu EI/(1 - \mu^2)$	
E	Young's modulus
G	shearing modulus of elasticity
h	thickness of wing
I	moment of inertia of skin per unit of width
I_r	moment of inertia of vertical web of rib
I_s	moment of inertia of vertical web of spar
i	number of a rib
j	number of a spar
Δ_i, Δ_j	increase in a function across ith rib and jth spar, respectively

M	bending moment
m	number of a bay along a spar; also a mass
n	number of a bay along a rib
Δ_m,Δ_n	increase in a function across mth bay of a spar and nth bay of a rib, respectively
P	concentrated load
q	shear flow
R	flexibility
t	thickness of skin
T	twisting moment
V	shear
w	deflection
x	spanwise coordinate
y	chordwise coordinate
z	vertical coordinate
α_m,α_n	angles center lines of a panel rotate through when panel is put in shear
β	rotation of a normal
γ	shearing strain
λ	length of a bay
μ	Poisson's ratio
ω	frequency
θ	slope of elastic axis

Subscripts:

ij	quantity in ith rib at jth spar
ji	quantity in jth spar at ith rib

in	quantity in ith rib at center of nth bay
jm	quantity in jth spar at center of mth bay
mn	quantity on spanwise cross section at center of cell mn
nm	quantity on chordwise cross section at center of cell mn
i	value in ith rib
j	value in jth spar
K	value in rib along line of support
m	value in mth bay along spar
n	value in nth bay along rib
x	value in web of spar
y	value in web of rib
xy	quantity having same value in rib or spar
max	maximum value

PHYSICAL ASSUMPTIONS OF THEORY

All stresses are assumed to be in the elastic range. The thickness of all webs is assumed to be sufficiently small that the variation of stress over the thickness may be neglected. It is assumed throughout the analysis that chordwise cross sections of the wing have a horizontal axis of symmetry. Some violation of this limitation can be tolerated in most cases without reducing significantly the accuracy of the solutions.

Two simplifying approximations must be introduced as follows:

(1) Since the depth of a wing varies in all directions, the shear flows in the skin on any cross section will have vertical components. The contributions of these vertical components to the shears on the cross sections are assumed to be negligible.

(2) Because of the variable depth of the wing, the normal stresses in the skin will have vertical components. The contributions which these vertical components make to the shears on the cross sections are assumed to be negligible.

As a result of the above assumptions the difference equations for the structure may be derived by considering a wing of constant depth without any loss of generality. The wing will also be assumed to have a constant chord as shown in figure 1(a). The wing may be supported at the face of the fuselage as shown. For purposes of analysis the original structure may be replaced by an idealized structure as indicated in figure 1(b). All of the normal stresses are assumed to be carried in flanges located at the junction of the ribs or spars and the skin. All connecting webs carry only shear flows.

EFFECT OF AXIS OF SYMMETRY OF CROSS SECTIONS

When a wing is acted upon by vertical loads or torsional loads and the cross sections have a horizontal axis of symmetry, it can be shown that the normal stresses have an antisymmetric distribution about the axis of symmetry. Hence the normal stresses may be considered to form bending moments just as in an ordinary plate. Similarly the shear flows in the skin may be shown to be antisymmetrical and, thus, may be considered to form twisting moments corresponding to ordinary plate theory. Since the internal stresses due to vertical or torsional loading may be expressed in terms of vertical shears, bending moments, and twisting moments, the equations which govern the structure take the form of plate equations.

VERTICAL EQUILIBRIUM OF AN ELEMENT

The first step in the development of the theory is to determine the relation between the internal shears and the applied load. The concentrated load acts at the intersection of the ith rib and the jth spar. A small portion of the wing surrounding this point may be removed for analysis. If the skin and idealized flanges are removed from the element, the remaining webs will appear as shown in figure 2. Only the vertical forces which act on the element are shown. In the idealized structure the shear in a rib or spar will be constant over the width of a cell, or bay. The first subscript indicates the member in which the shear acts and the second subscript indicates the bay in which the shear occurs. From figure 2 the equation of equilibrium is seen to be as follows:

$$V_{j(m+1)} - V_{jm} + V_{i(n+1)} - V_{in} + P_{ij} = 0 \qquad (1)$$

Differencing symbols will now be introduced. The symbol Δ_i indicates the jump in a function across the ith rib. The symbol Δ_j indicates

the jump in a function across the jth spar. An application of these operators to the shears yields the following formulas:

$$\Delta_i V_{jm} = V_{j(m+1)} - V_{jm} \tag{2a}$$

$$\Delta_j V_{in} = V_{i(n+1)} - V_{in} \tag{2b}$$

Substituting equations (2) into equation (1) gives

$$\Delta_i V_{jm} + \Delta_j V_{in} = -P_{ij} \tag{3}$$

This equation is a first-order difference equation.

EQUILIBRIUM OF MOMENTS ON AN ELEMENT

The next relation to be considered is that which holds between moments and shears. For this purpose an element of the wing must be considered as shown in figure 3. This element extends along the jth spar over the length λ_m of the mth bay. The only forces shown on the drawing are those which form couples having axes that are perpendicular to the spar. From figure 3 it is seen that the equation of equilibrium for moments is as follows:

$$M_{j(i+1)} - M_{ji} + T_{mn} - T_{m(n-1)} - \lambda_m V_{jm} = 0 \tag{4}$$

The twisting moment T_{mn} is the total twisting moment over the width of a cell rather than the twisting moment per unit of width which occurs in ordinary plate theory. The bending moment M_{ji} is the moment in the jth spar of the idealized structure at the point of intersection with the ith rib.

One may consider an element corresponding to the illustration of figure 3 which is oriented in the perpendicular direction. This element would contain the nth bay of a rib of length λ_n with the adjoining skin. Equilibrium of moments for couples having axes parallel to the x-axis gives the following equation:

$$M_{i(j+1)} - M_{ij} - T_{nm} + T_{n(m-1)} - \lambda_n V_{in} = 0 \tag{5}$$

Additional differencing symbols may now be introduced. The symbol Δ_m indicates the increase in a function across the mth bay of a spar. The symbol Δ_n indicates the increase in a function across the nth bay

of a rib. These operators may be applied to the bending moments to obtain the following formulas:

$$\Delta_m M_{ji} = M_{j(i+1)} - M_{ji} \tag{6a}$$

$$\Delta_n M_{ij} = M_{i(j+1)} - M_{ij} \tag{6b}$$

The operators Δ_i and Δ_j, which have been previously defined, may be applied to the twisting moments to obtain

$$\Delta_i T_{nm} = T_{nm} - T_{n(m-1)} \tag{7a}$$

$$\Delta_j T_{mn} = T_{mn} - T_{m(n-1)} \tag{7b}$$

Equations (6) and (7) may be substituted into equations (4) and (5) to obtain the following first-order difference equations:

$$\Delta_m M_{ji} + \Delta_j T_{mn} = \lambda_m V_{jm} \tag{8a}$$

$$\Delta_n M_{ij} - \Delta_i T_{nm} = \lambda_n V_{in} \tag{8b}$$

Since the shear flow in the skin on two perpendicular planes must be equal, there exists a simple relation between T_{mn} and T_{nm} which is expressed as follows:

$$\frac{T_{mn}}{\lambda_m} = -\frac{T_{nm}}{\lambda_n} \tag{9}$$

RELATION BETWEEN BENDING MOMENTS AND ROTATIONS OF NORMALS

The next step in the development of the theory is to form relations between bending moments and rotations of the normals to the middle surface. This requires a consideration of the deformation of a rib or spar which takes place when shearing strains are significant. In figure 4(a) there is shown a segment of a spar acted upon by shears and bending moments. A solid vertical line has been drawn normal to the elastic axis before distortion.

The spar is shown in its distorted position in figure 4(b). The original normal has rotated through an angle β_x and makes this angle with the vertical dashed line cd. The dashed line ab has been drawn perpendicular to the elastic axis in its deflected position. The original

normal makes an angle γ_x with ab where γ_x is the shearing strain in the web of the spar. The angle between ab and cd is equal to the slope of the elastic curve.

The normal strains in the idealized flanges are proportional to the rate of change of rotation of the original normals in the spar. Because of the Poisson ratio effect in the skin the rotation of the normals in the ribs will also contribute to the normal strains in the spars. Similar considerations can be given to a rib. This permits the writing of bending moments in terms of rotations of the normals in the ribs and spars.

The following equations may be written for the bending moments in the ith rib and the jth spar, respectively, at their intersection point:

$$M_{ij} = -D_{ij}\left(\frac{\partial \beta_y}{\partial y}\right)_{ij} - D_{ij}'\left(\frac{\partial \beta_x}{\partial x}\right)_{ij} \tag{10a}$$

$$M_{ji} = -D_{ji}\left(\frac{\partial \beta_x}{\partial x}\right)_{ij} - D_{ji}'\left(\frac{\partial \beta_y}{\partial y}\right)_{ij} \tag{10b}$$

The coefficient D_{ij} is the bending stiffness of the rib including the vertical web and the skin extending to the center of each adjacent cell. If I is the moment of inertia of the skin per unit of width and I_r is the moment of inertia of the vertical web of the rib, the formula for the bending stiffness of the rib becomes

$$D_{ij} = \lambda_i \frac{EI}{1 - \mu^2} + EI_r \tag{11a}$$

If I_s is the moment of inertia of the vertical web of the spar, the total bending stiffness of the spar becomes

$$D_{ji} = \lambda_j \frac{EI}{1 - \mu^2} + EI_s \tag{11b}$$

The Poisson ratio effect occurs only in the skin and hence the coefficients D_{ij}' and D_{ji}' are defined by the following equations:

$$D_{ij}' = \lambda_i \frac{\mu EI}{1 - \mu^2} \tag{12a}$$

$$D_{ji}' = \lambda_j \frac{\mu EI}{1 - \mu^2} \tag{12b}$$

For a nonuniform wing the values of I, I_r, and I_s may be computed at the point of intersection of the rib and spar. For better accuracy I may be computed as an average value over an appropriate area and I_r and I_s may be computed as average values over an appropriate length.

The derivatives which are contained in equations (10) must be replaced by finite differences. If β_{in} is the rotation of a normal in the ith rib at the center of the nth bay, the approximation to the first derivative is given by

$$\left(\frac{\partial \beta_y}{\partial y}\right)_{ij} = \frac{1}{\lambda_j}\left[\beta_{in} - \beta_{i(n-1)}\right] \tag{13a}$$

The corresponding equation for the spar is given by

$$\left(\frac{\partial \beta_x}{\partial x}\right)_{ij} = \frac{1}{\lambda_i}\left[\beta_{jm} - \beta_{j(m-1)}\right] \tag{13b}$$

If the appropriate differencing symbols are introduced, equations (13) become

$$\left(\frac{\partial \beta_y}{\partial y}\right)_{ij} = \frac{1}{\lambda_j} \Delta_j \beta_{in} \tag{14a}$$

$$\left(\frac{\partial \beta_x}{\partial x}\right)_{ij} = \frac{1}{\lambda_i} \Delta_i \beta_{jm} \tag{14b}$$

The finite differences which are given in equations (14) may be substituted into equations (10) to obtain the following equations relating bending moments and the rotations of the normals:

$$\frac{D_{ij}}{\lambda_j}\Delta_j\beta_{in} + \frac{D_{ij}'}{\lambda_i}\Delta_i\beta_{jm} = -M_{ij} \tag{15a}$$

$$\frac{D_{ji}}{\lambda_i}\Delta_i\beta_{jm} + \frac{D_{ji}'}{\lambda_j}\Delta_j\beta_{in} = -M_{ji} \tag{15b}$$

RELATION BETWEEN TWISTING MOMENTS AND ROTATIONS OF NORMALS

A relationship must now be derived between the twisting moments and the rotations of the normals to the middle surface. The twisting moments may be related to average values of the shearing strains in the skin panels. Simple relations may be found between these average strains and the rotations of the normals in the ribs and spars. These relations can be developed readily by reference to the idealized structure.

In figure 5 there is shown a panel of skin enclosed between two adjacent ribs and two adjacent spars. The position which the panel takes when the structure is loaded is shown in dashed lines. It will be assumed that the rotations of the normals in the ribs and spars are defined at midpoints which are indicated as A, B, C, and D in figure 5. The new positions which these four points take in the loaded structure are also shown. The components of displacement which these points take, in the direction of the members on which they are located, are indicated as a, b, c, and d.

The average shearing strain in the panel may be assumed to be equal to the change in angle made by the two center lines. These center lines rotate through the angles α_m and α_n. Hence the shearing strain in the panel is given by

$$\gamma_{mn} = \alpha_m + \alpha_n \tag{16}$$

These angles can be expressed in terms of the displacements and panel dimensions as follows:

$$\alpha_m = \frac{c - a}{\lambda_m} \tag{17a}$$

$$\alpha_n = \frac{b - d}{\lambda_n} \tag{17b}$$

The displacements can be expressed in terms of the rotations of normals as follows:

$$a = -\frac{h}{2}\beta_{in} \tag{18a}$$

$$b = -\frac{h}{2}\beta_{(j+1)m} \tag{18b}$$

$$c = -\frac{h}{2}\beta_{(i+1)n} \tag{18c}$$

$$d = -\frac{h}{2}\beta_{jm} \tag{18d}$$

Substituting equations (18) into equations (17) gives

$$\alpha_m = \frac{-h}{2\lambda_m}\left[\beta_{(i+1)n} - \beta_{in}\right] \tag{19a}$$

$$\alpha_n = \frac{-h}{2\lambda_n}\left[\beta_{(j+1)m} - \beta_{jm}\right] \tag{19b}$$

Introducing the appropriate differencing symbols gives

$$\alpha_m = \frac{-h}{2\lambda_m}\Delta_m\beta_{in} \tag{20a}$$

$$\alpha_n = \frac{-h}{2\lambda_n}\Delta_n\beta_{jm} \tag{20b}$$

Equations (20) may be substituted into equation (16) to obtain the following formula for the shearing strain:

$$\gamma_{mn} = -\frac{h}{2}\left[\frac{1}{\lambda_m}\Delta_m\beta_{in} + \frac{1}{\lambda_n}\Delta_n\beta_{jm}\right] \tag{21}$$

The twisting moments must now be expressed in terms of the shearing strains. The shearing stress is obtained from the strain by multiplying by the shearing modulus. The shear flow is then obtained by multiplying by the skin thickness.

$$q_{mn} = -\frac{Gth}{2}\left(\frac{1}{\lambda_m}\Delta_m\beta_{in} + \frac{1}{\lambda_n}\Delta_n\beta_{jm}\right) \tag{22}$$

The twisting moment per unit of width is obtained by multiplying by the depth of the wing. The total twisting moments for the cell are then obtained by multiplying by the length or width of the cell. The formulas thus obtained are

$$\frac{D_{mn}}{\lambda_m}\Delta_m\beta_{in} + \frac{D_{mn}}{\lambda_n}\Delta_n\beta_{jm} = -T_{mn} \tag{23a}$$

$$\frac{D_{nm}}{\lambda_m}\Delta_m\beta_{in} + \frac{D_{nm}}{\lambda_n}\Delta_n\beta_{jm} = T_{nm} \tag{23b}$$

The stiffness coefficients which appear in equations (23) may be computed from the following formulas:

$$D_{mn} = \lambda_m\frac{Gth^2}{2} = \lambda_m GI \tag{24a}$$

$$D_{nm} = \lambda_n\frac{Gth^2}{2} = \lambda_n GI \tag{24b}$$

RELATION BETWEEN DEFLECTIONS AND ROTATIONS OF NORMALS

It now remains to express the deflections in terms of the rotations of the normals by finite difference equations. Returning to figure 4 and considering similar conditions in the chordwise direction, the following two equations can be written:

$$\frac{\partial w}{\partial x} = \beta_x + \gamma_x \tag{25a}$$

$$\frac{\partial w}{\partial y} = \beta_y + \gamma_y \tag{25b}$$

The shearing strains are average values over the vertical webs of the ribs or spars. In the idealized structure these strains are constant over the shear webs.

The shearing strains are related to the shears by the following formulas:

$$\gamma_x = \frac{V_x}{GA_s} = \frac{V_x}{C_x} \tag{26a}$$

$$\gamma_y = \frac{V_y}{GA_r} = \frac{V_y}{C_y} \tag{26b}$$

In equations (26) A_s and A_r are the areas of vertical webs of the spars and ribs, respectively. Equations (26) may be substituted into equations (25) to obtain

$$\frac{\partial w}{\partial x} = \beta_x + \frac{V_x}{C_x} \tag{27a}$$

$$\frac{\partial w}{\partial y} = \beta_y + \frac{V_y}{C_y} \tag{27b}$$

It is now necessary to replace equations (27) by difference equations. The quantities on the right-hand side may be regarded as values at the center of a bay or they may be regarded as average values over a bay. The left-hand side may be replaced by finite differences to obtain the following equations:

$$\frac{1}{\lambda_m}\left[w_{(i+1)j} - w_{ij}\right] = \beta_{jm} + \frac{V_{jm}}{C_{jm}} \tag{28a}$$

$$\frac{1}{\lambda_n}\left[w_{i(j+1)} - w_{ij}\right] = \beta_{in} + \frac{V_{in}}{C_{in}} \tag{28b}$$

In equations (28) the shearing stiffnesses may be computed at the center of the bay although better accuracy will be obtained by computing average values over the bays. Introducing appropriate differencing symbols into equations (28) gives

$$\frac{1}{\lambda_m}\Delta_m w_{ij} = \beta_{jm} + \frac{V_{jm}}{C_{jm}} \tag{29a}$$

$$\frac{1}{\lambda_n}\Delta_n w_{ij} = \beta_{in} + \frac{V_{in}}{C_{in}} \tag{29b}$$

The complete solution is now defined by nine first-order difference equations. The nine unknowns consist of six internal force quantities (shears, bending moments, and twisting moments) and three displacement quantities (deflections and rotations of normals). The first-order equations may be combined to form equations of higher order. This would be necessary if the solution were to be computed on a digital computer. However, when the solution is to be computed on an analog machine the equations may be left in their present form. Coupled circuits may be designed in which the voltages and currents are related by first-order difference equations which have the same mathematical form as the structural equations. From these circuits one may read any one of the nine unknown quantities independently.

VIBRATION MODES

The natural vibration modes and frequencies of the wing may be easily determined by replacing the distributed mass by an equivalent set of concentrated masses. These masses must be considered as being located at the intersection points of the ribs and spars. Using D'Alembert's principle and assuming sinusoidal motion at a frequency ω, the concentrated load becomes

$$P_{ij} = \omega^2 m_{ij} w_{ij} \tag{30}$$

Equation (30) may be substituted into equation (3) to obtain

$$\Delta_i V_{jm} + \Delta_j V_{in} = -\omega^2 m_{ij} w_{ij} \tag{31}$$

Equation (31) must be used in place of equation (3) for vibration analysis. All other equations remain unchanged.

BOUNDARY CONDITIONS

When the computations are to be made on an analog computer the boundary conditions on free edges may be stated directly in terms of force quantities. In stating the boundary conditions for quantities which are defined at the center of a bay or a cell, it is convenient to introduce a row of imaginary cells surrounding the plan form of the

wing as shown in figure 6. For convenience it will be assumed that the plan form has double symmetry and the boundary conditions will be stated for the first quadrant.

If n_{max} is the maximum value of n on the plan form, the exterior row of imaginary cells in front of the leading edge may be numbered $n_{max} + 1$ as shown in the figure. Similarly the row of cells beyond the wing tip is numbered $m_{max} + 1$. The rib at the tip is numbered i_{max} (maximum value of i) and the spar at the leading edge is numbered j_{max} (maximum value of j). The rib at the line of support is numbered K. In terms of the above-defined symbols the boundary conditions can be expressed as follows:

Line of support:

$$w_{Kj} = 0 \tag{32}$$

Wing tip:

$$V_{j(m_{max} + 1)} = 0 \tag{33a}$$

$$M_{j(i_{max})} = 0 \tag{33b}$$

$$T_{n(m_{max} + 1)} = 0 \tag{33c}$$

Leading edge:

$$V_{i(n_{max} + 1)} = 0 \tag{34a}$$

$$M_{i(j_{max})} = 0 \tag{34b}$$

$$T_{m(n_{max} + 1)} = 0 \tag{34c}$$

DESIGN OF ANALOGOUS CIRCUIT

An explanation of the design of the analogous circuit will be given in a manner corresponding to the treatment of beam analogies which is contained in reference 1. Since the design procedure has been described in complete detail in reference 1, the present design will be stated more briefly. Since the structural equations have the same form as plate equations the analogous circuits will be approximately the same as those given by MacNeal (reference 2). The only difference will be due to the allowance for the effect of shearing strains upon deflections.

In reference 1 the structural quantities and the electrical quantities were represented by completely separate sets of symbols. In the present paper the structural symbols will also be used as electrical symbols. Thus it will not be necessary to write additional equations for the electrical circuit. For convenience in the discussion of the circuit the structural equations which govern the problem are repeated in a group as follows:

$$\Delta_i V_{jm} + \Delta_j V_{in} = -P_{ij} \tag{3}$$

$$\Delta_m M_{ji} + \Delta_j T_{mn} = \lambda_m V_{jm} \tag{8a}$$

$$\Delta_n M_{ij} - \Delta_i T_{nm} = \lambda_n V_{in} \tag{8b}$$

$$\frac{T_{mn}}{\lambda_m} = -\frac{T_{nm}}{\lambda_n} \tag{9}$$

$$\frac{D_{ij}}{\lambda_j} \Delta_j \beta_{in} + \frac{D_{ij}'}{\lambda_i} \Delta_i \beta_{jm} = -M_{ij} \tag{15a}$$

$$\frac{D_{ji}'}{\lambda_j} \Delta_j \beta_{in} + \frac{D_{ji}}{\lambda_i} \Delta_i \beta_{jm} = -M_{ji} \tag{15b}$$

$$\frac{D_{mn}}{\lambda_n} \Delta_n \beta_{jm} + \frac{D_{mn}}{\lambda_m} \Delta_m \beta_{in} = -T_{mn} \tag{23a}$$

$$\frac{D_{nm}}{\lambda_n} \Delta_n \beta_{jm} + \frac{D_{nm}}{\lambda_m} \Delta_m \beta_{in} = T_{nm} \tag{23b}$$

$$\frac{1}{\lambda_m} \Delta_m w_{ij} = \beta_{jm} + \frac{V_{jm}}{C_{jm}} \tag{29a}$$

$$\frac{1}{\lambda_n} \Delta_n w_{ij} = \beta_{in} + \frac{V_{in}}{C_{in}} \tag{29b}$$

It is seen that equation (3) expresses a relation between force quantities and hence is represented electrically by an application of Kirchhoff's law to a nodal point. This nodal point is shown in figure 7 where the structural equation is also given. The currents are

designated with structural symbols so that the structural equation may be interpreted as an electrical equation.

The next equation to be considered is equation (8a). This again calls for an application of Kirchhoff's law at a node and is illustrated in figure 8. In this figure it will be noted that the "loading current" $\lambda_m V_{jm}$ proceeds from a transformer through a resistance. This resistance is required to allow for the effect of shearing strains upon the deflections. Equation (8b) is of a similar nature and the analogous node is shown in figure 9.

Three different nodal points have been illustrated. Each of these nodes must occur in a different planar circuit. Hence three planar circuits must be designed and interconnected by means of transformers. A panel of the shear circuit is shown in figure 10. In this circuit the voltages represent deflections and the currents represent shears.

The design of the other two planar circuits requires the introduction of additional circuit elements. The next structural equations to be considered are equations (15). For more convenient electrical representation these equations are solved for the differences in rotations in terms of bending moments. The result of such a solution may be written as follows:

$$\Delta_i \beta_{jm} = -R_x M_{ji} + R_{xy} M_{ij} \tag{35a}$$

$$\Delta_j \beta_{in} = R_{xy} M_{ji} - R_y M_{ij} \tag{35b}$$

The circuit elements corresponding to equations (35a) and (35b) are shown in figures 11(a) and 11(b), respectively. In order to see more clearly that the voltages and currents shown in figure 11 are related by equations (35) one may rewrite equations (35) in the following form:

$$\Delta_i \beta_{jm} = -\left(R_x - R_{xy}\right) M_{ji} - R_{xy}\left(M_{ji} - M_{ij}\right) \tag{36a}$$

$$\Delta_j \beta_{in} = -R_{xy}\left(M_{ij} - M_{ji}\right) - \left(R_y - R_{xy}\right) M_{ij} \tag{36b}$$

Equation (36a) may be immediately checked by an inspection of figure 11(a). In order to see that equation (36b) is valid one must use the transformer laws. These laws have been illustrated in reference 1. One-half of a transformer is shown in figure 11(a) and the other half of the same transformer is shown in figure 11(b). This transformer has a 1:1 turns ratio. The plus and minus signs indicate

the polarity (or phase) of the terminal voltages. The manner in which the circuit elements of figure 11 are coupled is illustrated in figure 12.

The next equations to be considered are equations (23). For convenience in designing the circuit these equations may be written in the following modified form:

$$\Delta_n \beta_{jm} + \frac{\lambda_n}{\lambda_m} \Delta_m \beta_{in} = - \frac{\lambda_n}{D_{mn}} T_{mn} \tag{37a}$$

$$\Delta_n \beta_{jm} + \frac{\lambda_n}{\lambda_m} \Delta_m \beta_{in} = \frac{\lambda_n}{D_{nm}} T_{nm} \tag{37b}$$

Equations (37a) and (37b) are not independent since the right-hand sides are related as shown by equation (9). A circuit element is shown in figure 13(a) in which the voltages and currents are related by equation (37a). The associated circuit element is shown in figure 13(b). The manner in which the elements of figure 13 are coupled is shown in figure 14. A verification of equation (37a) as an electrical equation requires an application of the transformer law for voltages. Equation (9) is a direct statement of the transformer law for currents. It is seen from these equations that the ratio λ_n/λ_m must be the transformer turns ratio.

The next equations to be considered are equations (29). These equations may be interpreted as electrical equations by referring to figures 15 and 16. Figure 15 shows the transformer connection between the shear circuit wherein voltages are deflections and the spanwise-bending-moment circuit wherein the voltages are rotations of the normals in the spars. The point at which the voltage corresponds to the slope of the elastic curve of the spar is indicated as θ_{jm}. Figure 16 shows a similar connection between the shear circuit and the chordwise-bending-moment circuit.

A panel of the circuit for spanwise bending moments is shown in figure 17. A similar circuit for chordwise bending moments is shown in figure 18. Complete assembled circuits are shown in reference 2.

CONCLUDING REMARKS

A theoretical method of analysis has been developed whereby the stresses and deflections may be determined for a thin supersonic wing

of low aspect ratio. It is assumed that chordwise cross sections of the wing have a horizontal axis of symmetry. This permits the reduction of the solution to the form of plate theory. In order to carry out the analysis on an analog computer the theory is expressed in terms of first-order difference equations. The analogous electrical circuits are also derived.

California Institute of Technology
Pasadena, Calif., February 5, 1952

REFERENCES

1. Benscoter, S. U., and MacNeal, R. H.: An Introduction to Electrical Circuit Analogies for Beam Analysis. NACA TN 2785, 1952.

2. MacNeal, R. H.: The Solution of Elastic Plate Problems by Electrical Analogies. Jour. Appl. Mech., vol. 18, no. 1, March 1951, pp. 59-67.

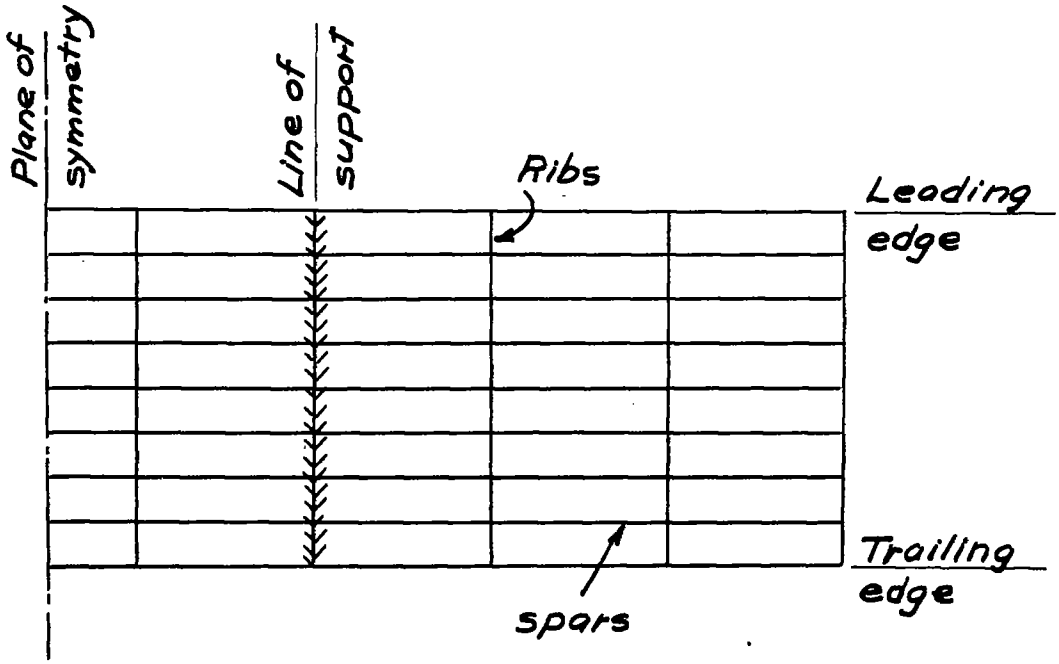

(a) Layout of ribs and spars.

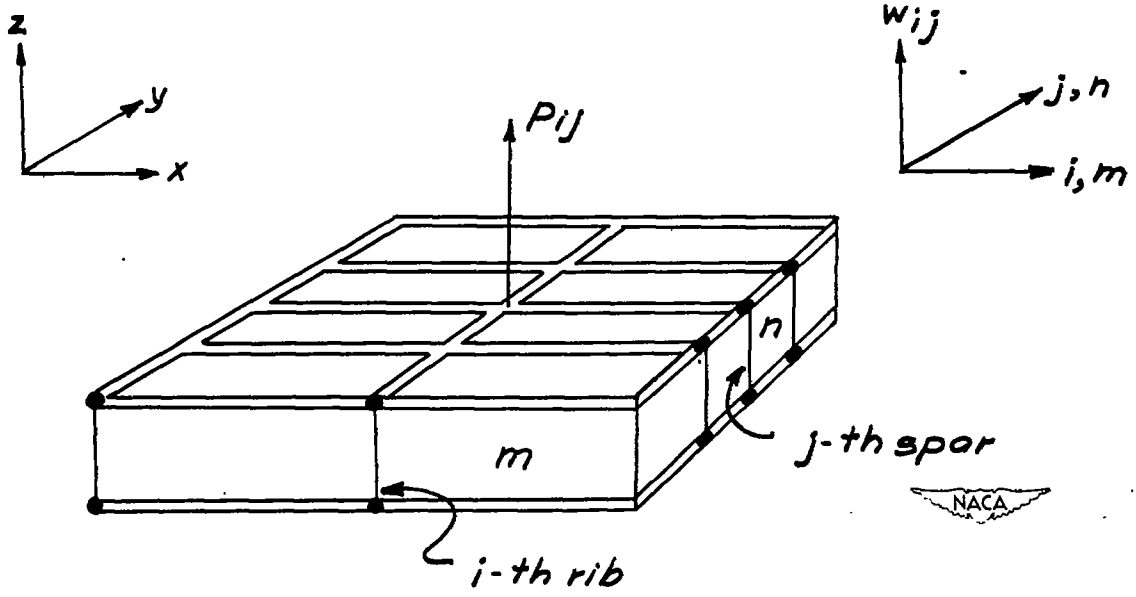

(b) Idealized structure.

Figure 1.- Uniform multicell plate.

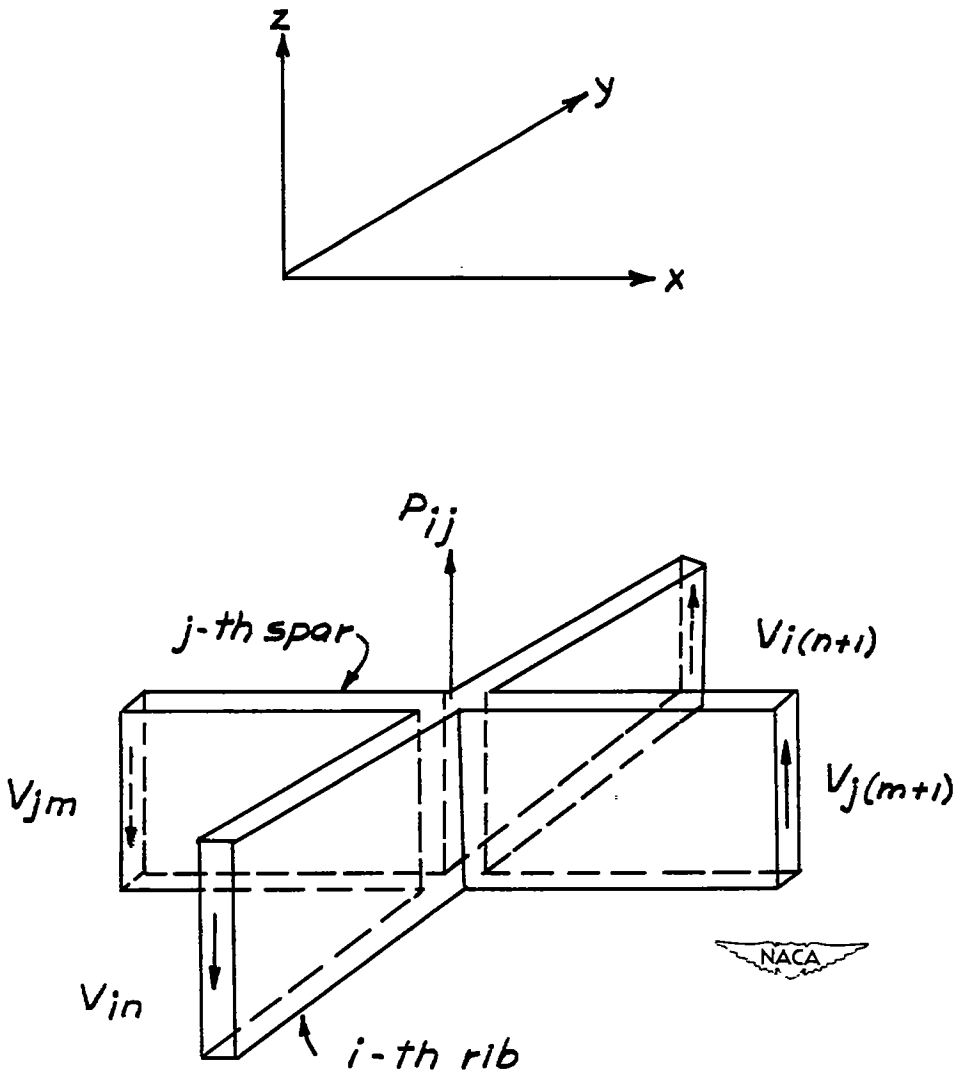

Figure 2.- Vertical forces acting on element of plate.

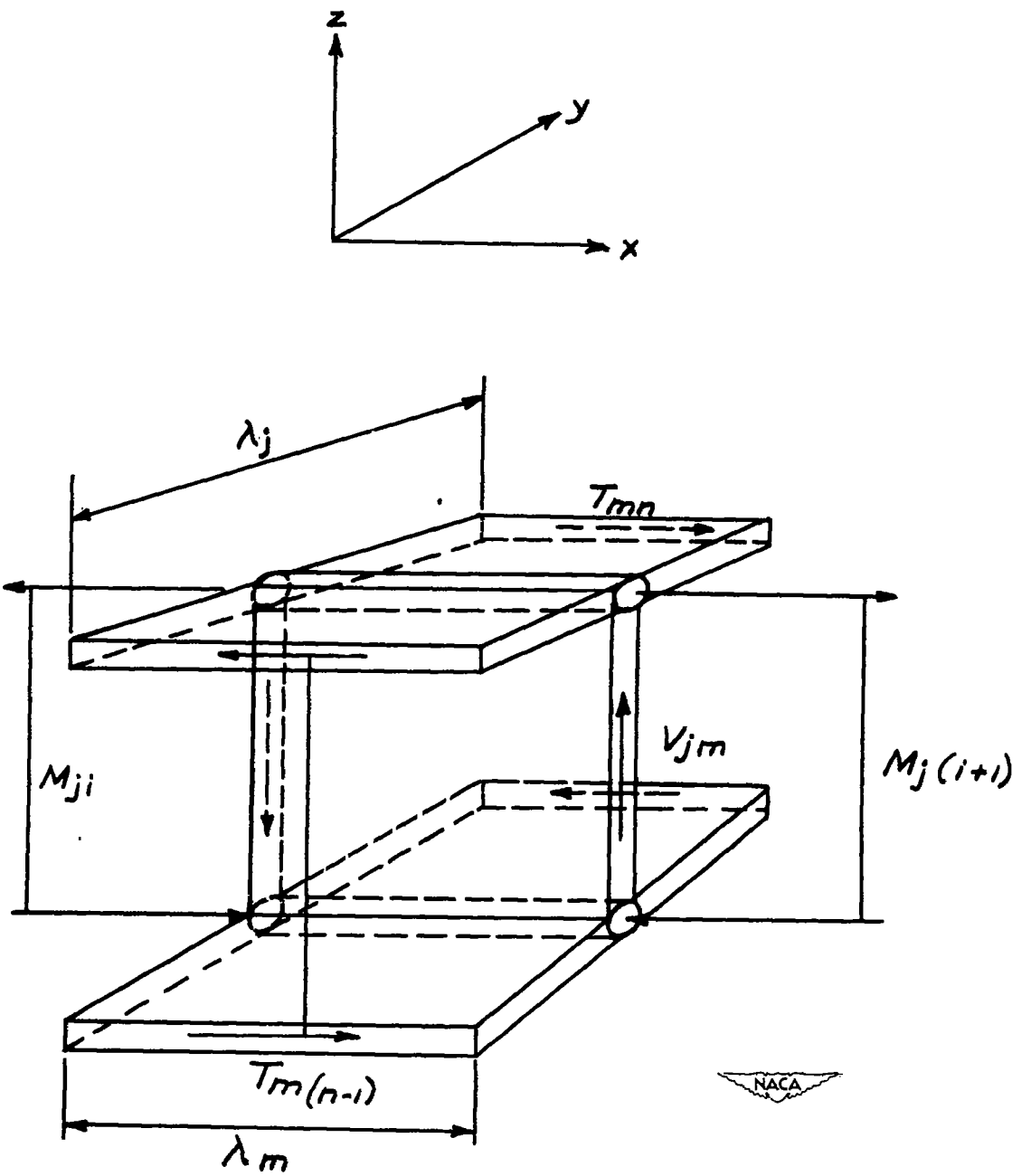

Figure 3.- Spanwise moments acting on element of plate.

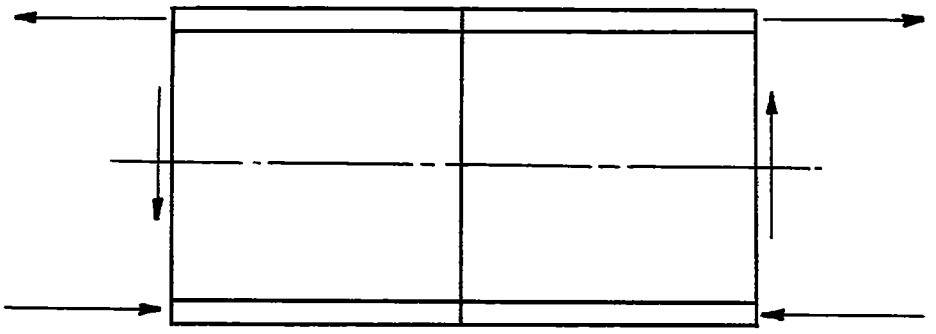

(a) Segment before distortion.

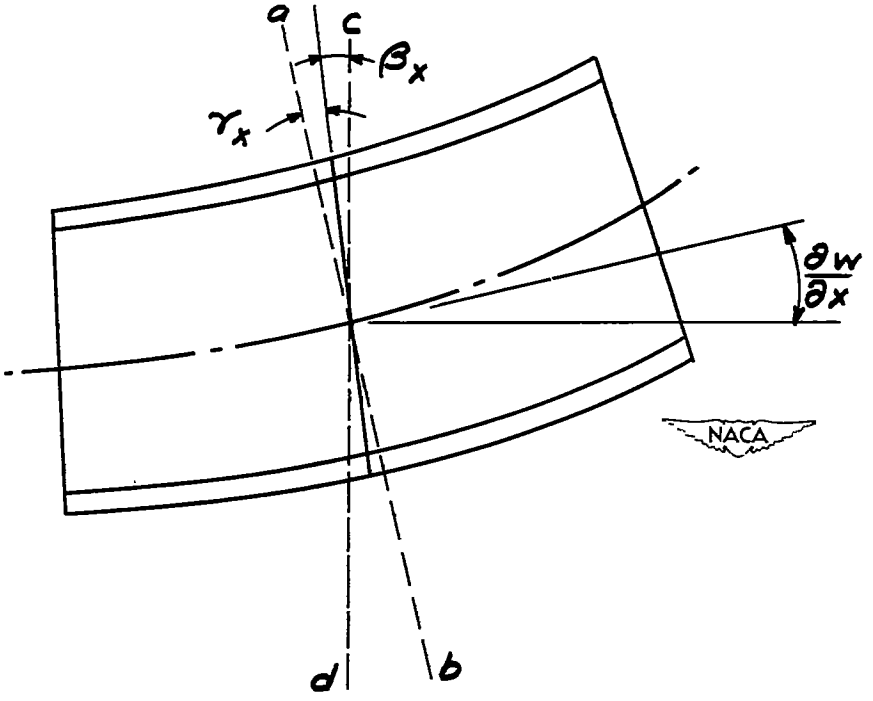

(b) Segment after distortion.

Figure 4.- Distortions of a segment of a spar.

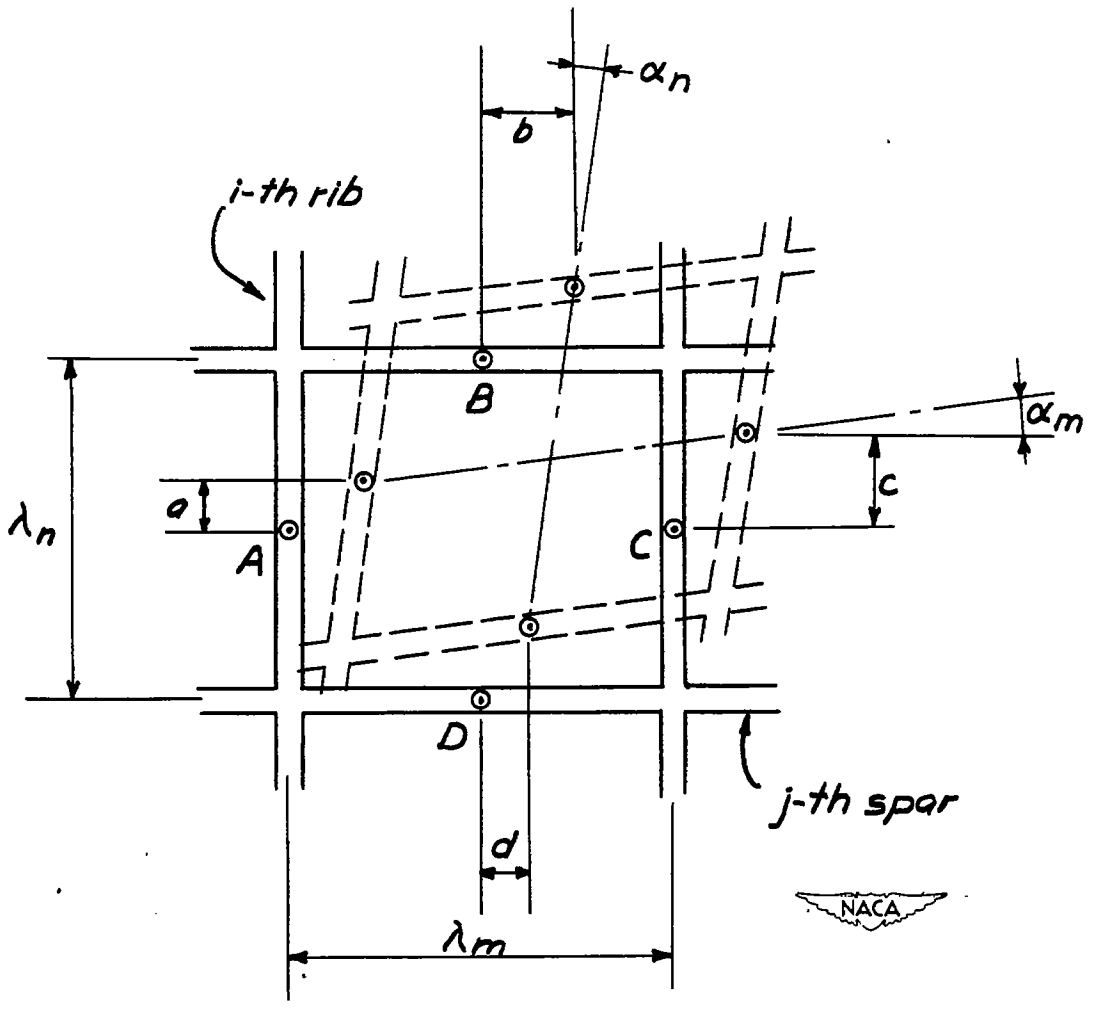

Figure 5.- Shearing distortion of a skin panel.

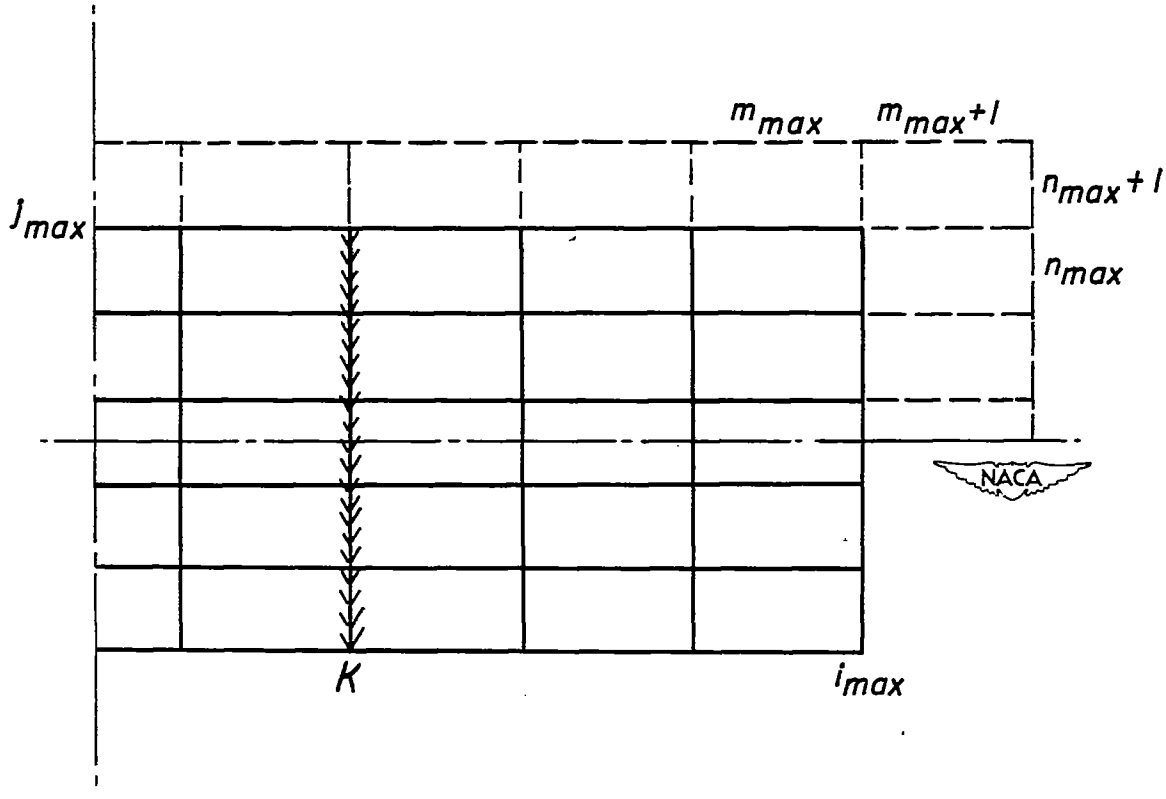

Figure 6.- Symbols required for statement of boundary conditions.

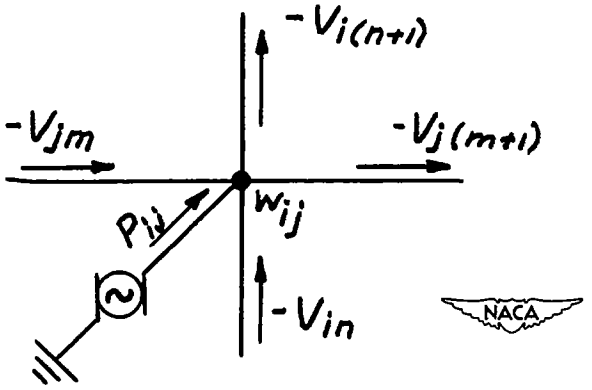

Figure 7.- Nodal point in shear circuit. $\Delta_i V_{jm} + \Delta_j V_{in} = -P_{ij}$.

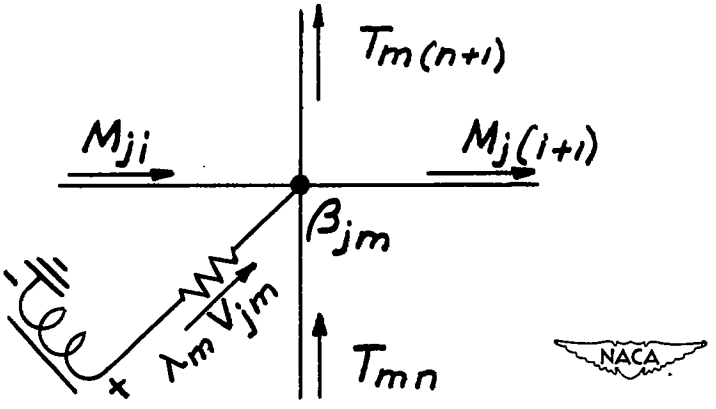

Figure 8.- Nodal point in spanwise-bending-moment circuit.
$\Delta_m M_{ji} + \Delta_j T_{mn} = \lambda_m V_{jm}$.

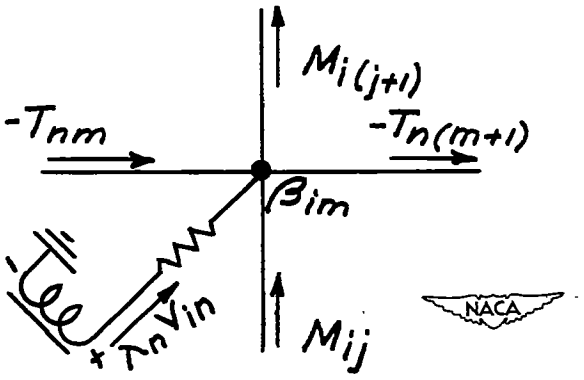

Figure 9.- Nodal point in chordwise-bending-moment circuit. $\Delta_n M_{ij} - \Delta_i T_{nm} = \lambda_n V_{in}$.

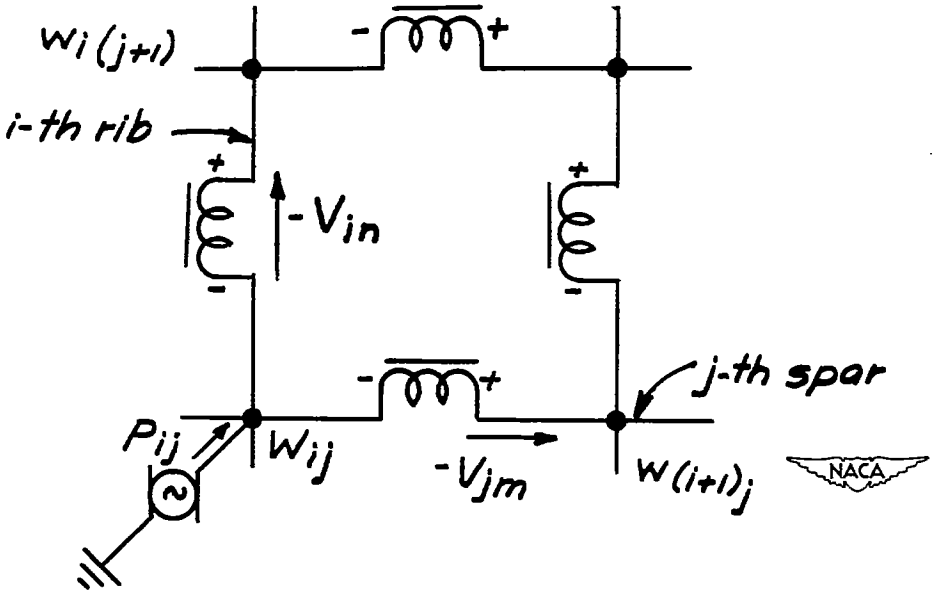

Figure 10.- Panel of circuit for shears and deflections.

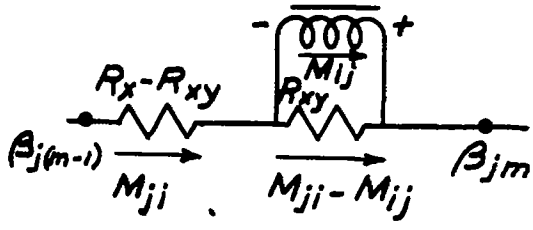

(a) Spanwise bending moments.
$\Delta_i\beta_{jm} = -R_xM_{ji} + R_{xy}M_{ij}$.

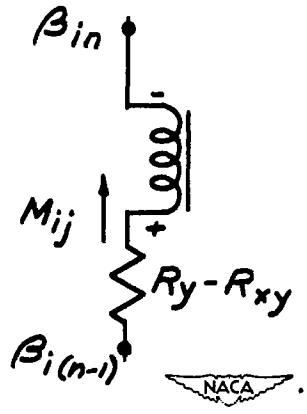

(b) Chordwise bending moments.
$\Delta_j\beta_{in} = R_{xy}M_{ji} - R_yM_{ij}$.

Figure 11.- Circuits for bending moments.

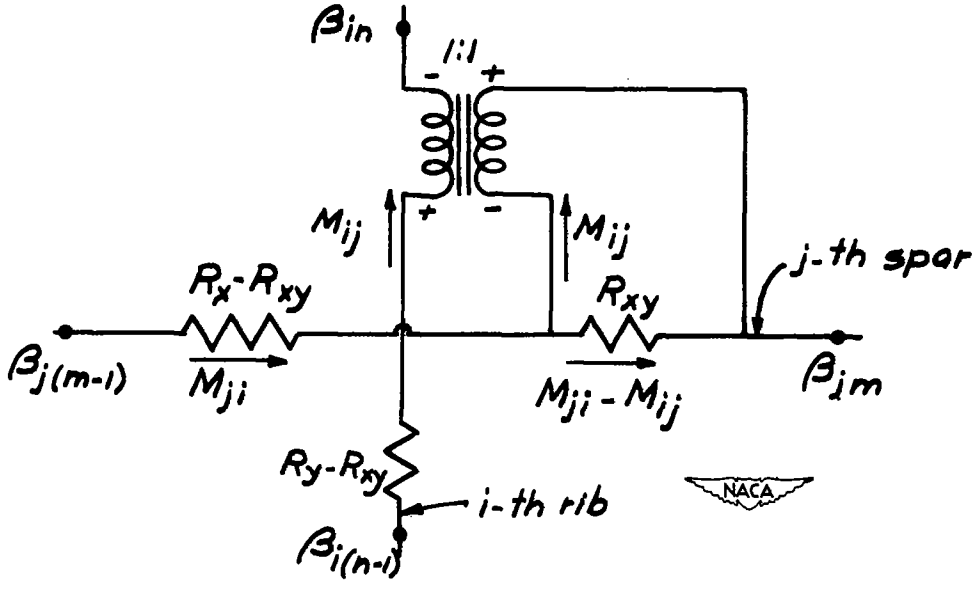

Figure 12.- Coupling of circuits for bending moments.

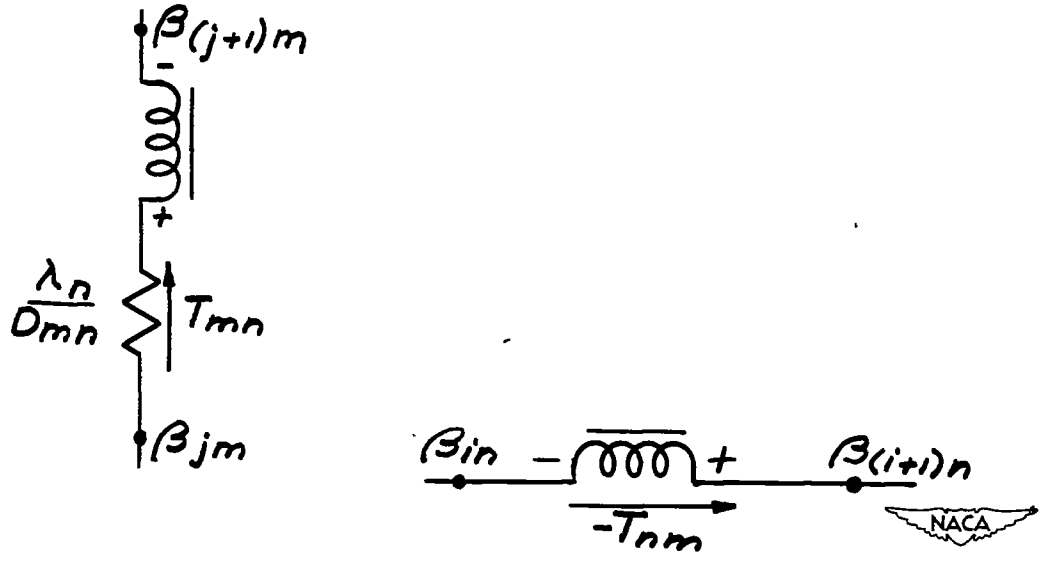

(a) Twisting moment on spanwise cross section.

(b) Twisting moment on chordwise cross section.

Figure 13.- Circuits for twisting moments. $\Delta_n\beta_{jm} + \frac{\lambda_n}{\lambda_m}\Delta_m\beta_{in} = -\frac{\lambda_n}{D_{mn}}T_{mn}$;

$$T_{nm} = -\frac{\lambda_n}{\lambda_m}T_{mn}.$$

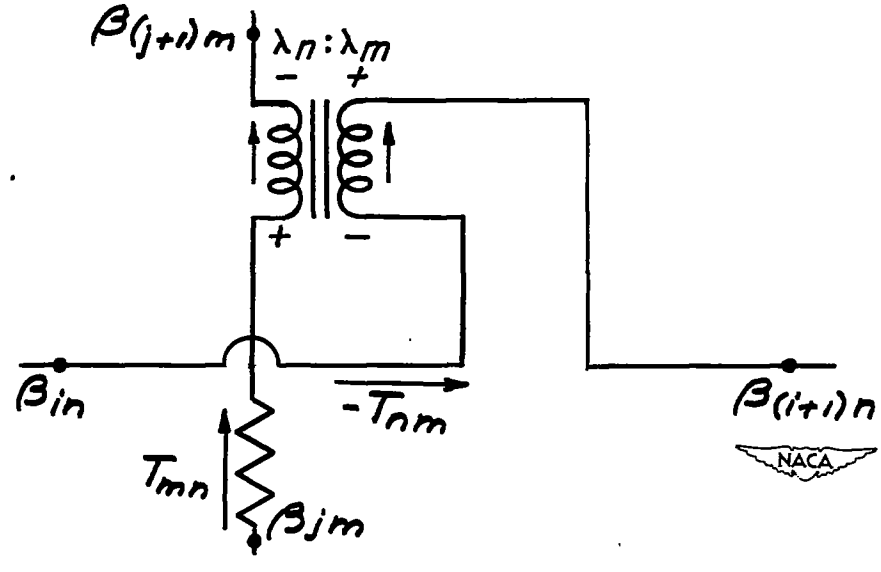

Figure 14.- Coupling of circuits for twisting moments.

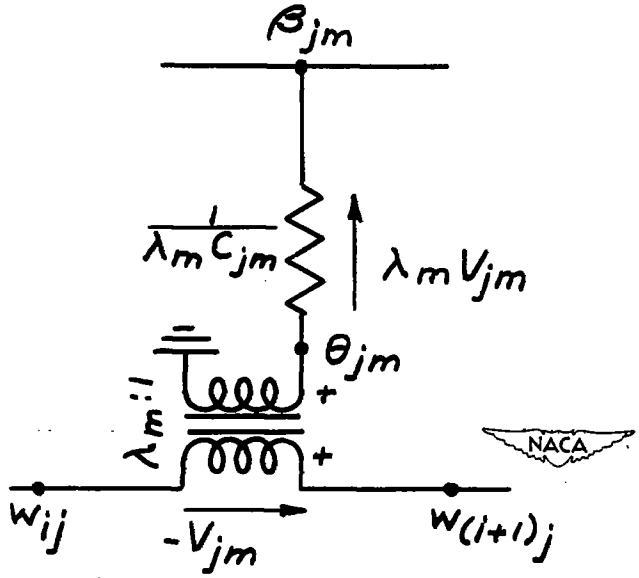

Figure 15.- Relation between deflections and spanwise slopes.

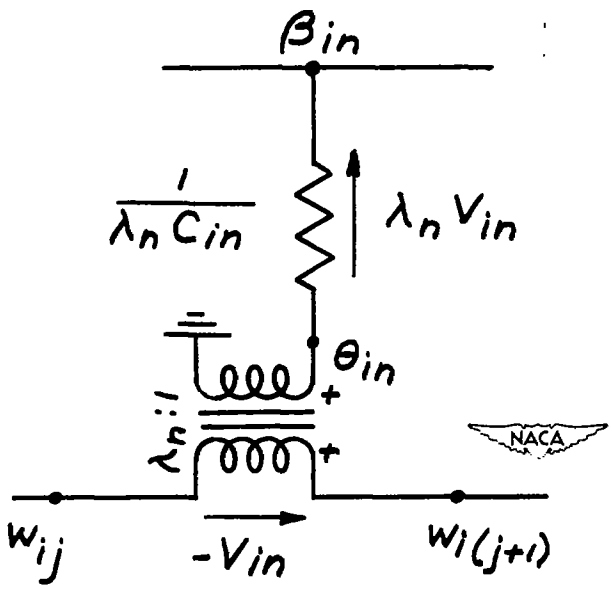

Figure 16.- Relation between deflections and chordwise slopes.

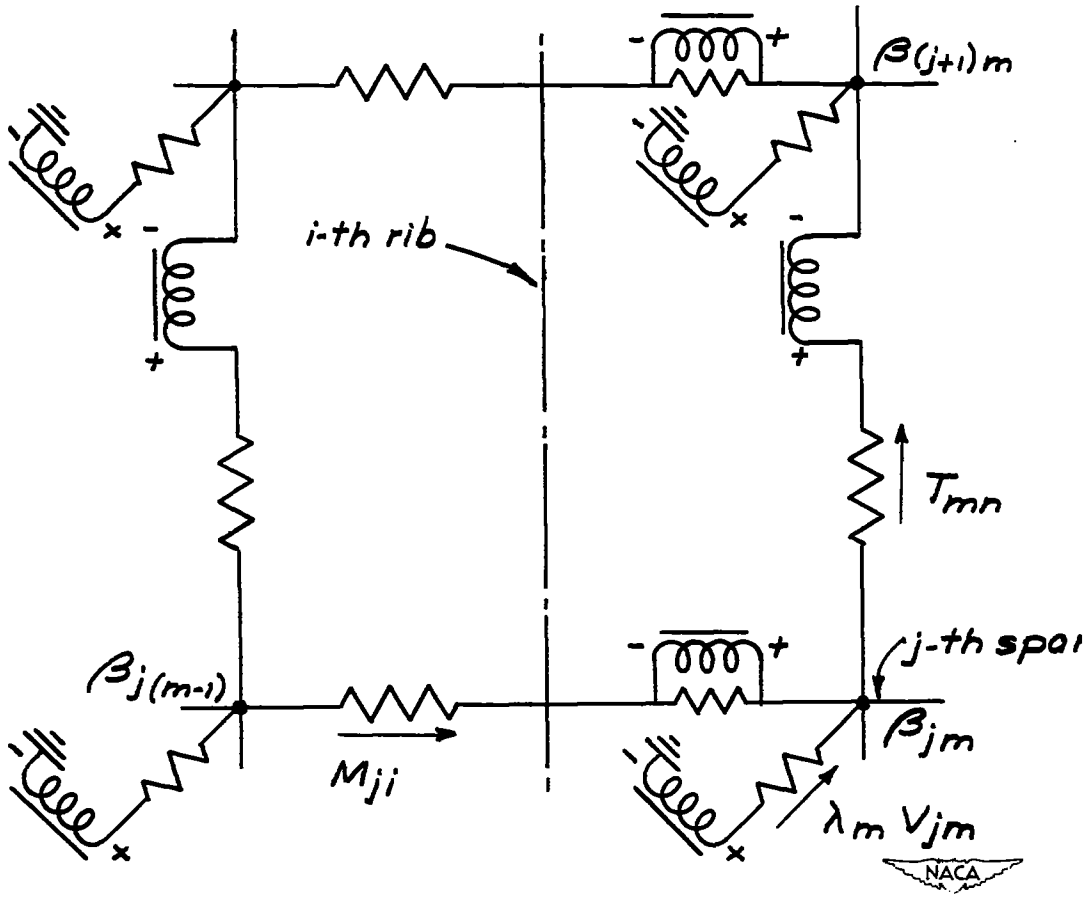

Figure 17.- Panel of circuit for spanwise bending moments.

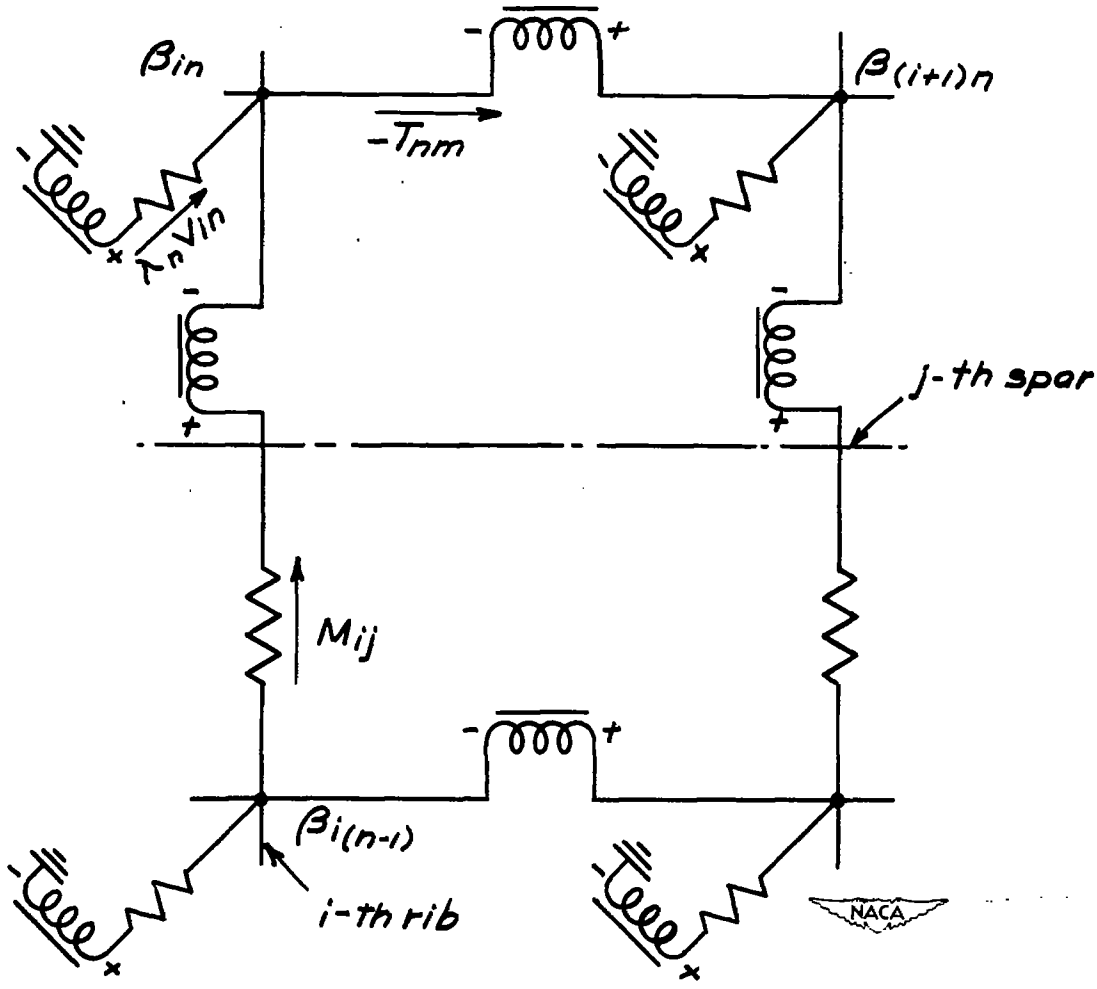

Figure 18.- Panel of circuit for chordwise bending moments.